CANCELING ECHOES DISTORTED BY SATELLITE TRANSPONDERS

S. Jayasimha and P. Jyothendar

Signion Systems Ltd.
20, Rockdale Compound
Somajiguda, Hyderabad-500082
e-mail: info@signion.com

ABSTRACT

We describe the design and performance for a canceller (applied to "carrier-in-carrier" satellite communications) of a distorted echo signal superposed on a desired signal, providing both its convergence and steady-state behaviors in the presence of TWTA transponder induced distortion.

1. INTRODUCTION

Each direction of a conventional duplex radio link uses different carrier frequencies. If both directions used the same frequency, canceling the undesired transmit signal, 4-5 orders larger at the receive antenna than the desired signal, becomes very difficult. However, in "carrier-in-carrier" satellite radio relays (i.e., with overlapped up- and down-link frequency bands as in Figure 1), where transmit and receive antenna dishes point narrow beams at the geo-stationary satellite, the returned transmit signal (echo) to desired signal ratio is nominally the product of near- to far-ends' antenna gain ratio, Γ, and the ratio of required carrier-to-noise (C/N) ratios.

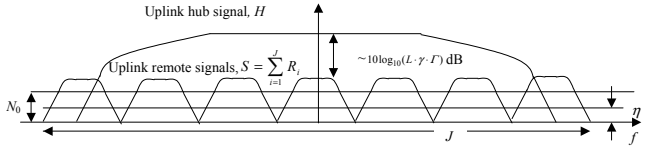

$$\frac{(C/N_0)_H}{(C/N_0)_R} \sim 10\log_{10}(L\cdot\gamma) \text{ dB, where } \gamma=\frac{(E_b/N_o)_H}{(E_b/N_o)_R}\cdot\frac{\log_2 M_H}{\log_2 M_R},\ M_x=2^{BR_x/BW_x};$$

(BR_x, BW_x are bitrate and bandwidth of signal x)

η-Noise added due inter-modulation distortion (desire to keep this below N_0),
L=bit rate ratio of H and R, J is number of equi-bandwidth carriers in S.

Figure 1. Up-linked hub and remote signals (superposed and amplified by a satellite transponder)

VSAT networks typically consist of one or more earth station with large diameter antennas (called "hubs") that link (to each other, as well as to terrestrial networks) earth stations with smaller antennas (called "remote stations"). A hub usually modulates a single carrier, H, at a high rate to transmit data to remote stations using time division multiple access, while it receives relatively low rate data signals, R, from remote stations at different carriers. Thus, C/N ratios are higher for hub-emanating signals as compared to those from the remote stations (for identical modulation, their data rate ratio). Since the returned transmit signal is much weaker at remote stations than the intended receive signal (due to both the lower transmit signal power as well as lower antenna gain), no cancellation of the unwanted transmit signal is required. However, the hub (see Figure 2) must subtract out a distorted (for transponders with memory-less non-linear amplitude and phase responses with respect to input signal amplitude), scaled and delayed version (H_d) of the known transmit signal[1] (H) from the received aggregate signal (A) to produce the composite remote stations' signals[2] (R) plus noise and inter-modulation products.

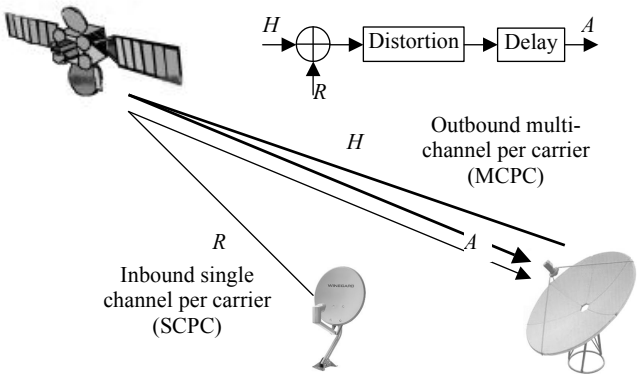

Figure 2. Desired remote signals added on hub's distorted, scaled and delayed transmit signal

With hybrid and PCM codec induced echo-path distortion compensation absent, echo suppression in telephony (e.g., line [1] and acoustic echo [2] cancellation) is limited to 30-35dB. Representing a memory-less non-linearity as a polynomial (in its input) and adapting its coefficients [3] allows greater suppression. However, this method is not amenable to satellite echo cancellers because transponder distortion, with both normalized gain and phase approximately quadratic (at sufficient back-off) with respect to amplitude, cannot be approximated as a small-order, e.g., quadratic [4, 5], filter.

Details of a method to cancel satellite echoes are described in [6], such as delay (to ±½ sample) and Doppler acquisition, time (including fractional sample) delay and Doppler tracking, also applicable to canceling distorted echoes, are not repeated here. Rather, we focus on increasing suppression by incorporating low-complexity distortion compensation into the echo canceller described in [6] as in Figure 3.

---

[1] Linear power amplifiers are generally used at the hub.

[2] The peak-to-rms ratio of N remote stations' composite signal, R, may be $\sqrt{N}$ larger than a constituent R_k's. Assume that $\max|R_k|$ and N are chosen so that H determines distortion rather than R.

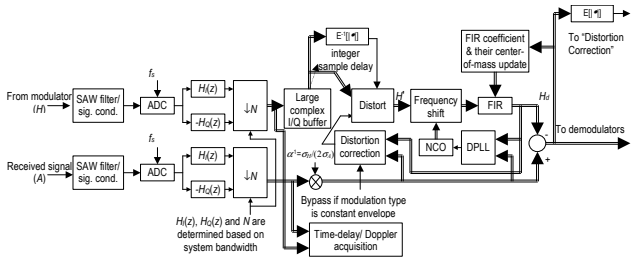

Figure 3. Distortion compensating echo canceller

Both signals H and A are digitized at IF, quadrature filtered and decimated (by a factor consistent with signal bandwidth) to obtain complex base-band samples. The base-band signal H enters a DRAM buffer that accounts for integer sample delay (that is initially acquired and subsequently tracked), then distorted prior to being frequency shifted and fractional-sample delayed (by an adaptive FIR filter), before being subtracted from A to yield the base-band signals, R. This signal may then be up-converted back to IF for presentation to remote-station demodulators/ decoders, where other processing (e.g., [7,8]) can further mitigate distortion effects on each R.

2. DISTORTION ESTIMATION

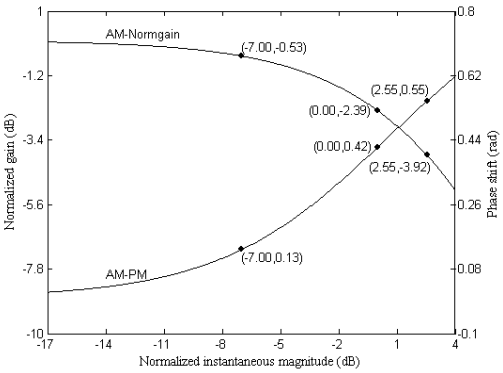

Figure 4. TWTA AM-Normgain and AM-PM responses (unshaped 16-QAM amplitudes marked at –7dB IBO)

For a TWTA transponder, the Saleh model [9] base-band amplitude (AM-AM) and phase (AM-PM) responses are $A(r)=\alpha_a \cdot r/(1+\beta_a \cdot r^2)$ and $\phi(r)=\alpha_\phi \cdot r^2/(1+\beta_\phi \cdot r^2)$ respectively; Figure 4 shows AM-normalized gain (hereafter "AM-Normgain" or $G_N(r)=[1+\beta_a \cdot r^2]^{-1}$ for TWTA) and AM-PM characteristics, when average signal power is –7dB IBO, using typical parameters α_a=2.0, β_a=1.0, α_ϕ=2.5 and β_ϕ=2.8, with instantaneous magnitude normalized to rms value. For GaAsFETs, the Ghorbani [10] model for AM-AM distortion, with $A(r)=[(x_1 \cdot r^{x_2})/(1+x_3 \cdot r^{x_2})]+x_4 \cdot r$, may be used while Saleh's AM-PM distortion may be retained to obtain a 6 (rather than Ghorbani's 8) parameter model. Typical parameters are x_1=8, x_2=1.5, x_3=6.5, x_4=-0.1, α_ϕ=5.5 and β_ϕ=13. The AM-AM for SSPA [11] model is $A(r)=r/(1+r/\alpha_a)^{0.5}$ with α_a=0.4, $\phi(r)$=0.

In all cases, the AM-Normgain and AM-PM characteristics, which vary slowly, may be derived from the (time aligned) LMS output signal, H_d, and the received aggregate signal A (as in Figure 2) via an iterative distortion correction process, depicted in Figure 5, which is bypassed unless H_d's variance approximately equals A's (i.e., high H_d/R ratio[3]).

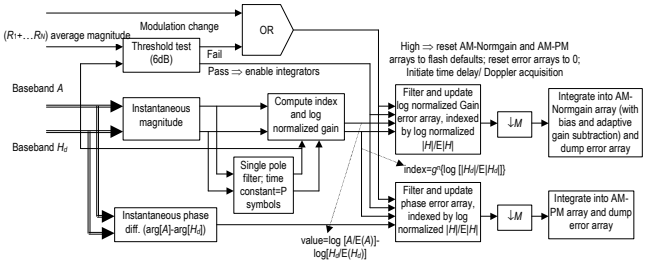

Figure 5. Distortion correction

Figure 5 describes the process[4] by which the LMS delay equalizer output, H_d, time-aligned to A, is used to iteratively update estimates of AM-Normgain and AM-PM curves (e.g., ultimately settling at Figure 4's curves). Log normalized $|H|$ is inferred from log normalized $|H_d|$ through fixed-point iteration in the AM-Normgain array, f, i.e., if we define $g\{\bullet\}=\{\log(|H_d|/\mathrm{E}|H_d|)-f(\bullet)\}$, then fixed-point iteration is $g\{g\{\ldots\}\}=g^n(\bullet)$ until $g^n\{\log(|H_d|/\mathrm{E}|H_d|)\}+f\{g^n[\log(|H_d|/\mathrm{E}|H_d|]\}$ $-\log[|H_d|/\mathrm{E}|H_d|]$ is less than a resolution threshold[5] (e.g., 1/6 dB) or $g^n\{\log(|H_d|/\mathrm{E}|H_d|\}$ exceeds an upper limit (e.g., 4dB).

The AM-Normgain correction array, indexed by log normalized $|H|$, is updated by filtering (e.g., using a dc unity-gain, first-order filter) $\log(|A|/\mathrm{E}|A|)-\log(|H_d|/\mathrm{E}|H_d|)$. This array is periodically integrated into the AM-Normgain array, after bias subtraction[6] (Figure 6) and adaptive filter gain compensation (see Section 4 and appendices I-III). AM-Phase correction array update is based on $\arg(A)-\arg(H)$. R's envelope estimate is also biased by excess mean square error (MSE) from the fractional sample delay adaptation (details in section 3); thus, R's envelope divided by $(1+\mu L \sigma_{H'}{}^2)^{0.5}$ is N's.

---

[3] So that inter-modulation products [12] (dominated, for carrier-in-carrier systems, by in-band $H_d \cdot R$ terms), that bias AM-Normgain and AM-PM estimates, may be neglected.

[4] To reduce computational rate by M, H_d and A are decimated by M (>1 and gcd[M, lcm(f_s, f_b)]=1, f_s and f_b being sample and baud rates respectively), at the distortion correction rate's expense.

[5] A convex AM-Normgain ensures the iterative process's termination.

[6] The non-central distribution $f(x,y)=\frac{e^{-\left[(x-\eta)^2+y^2\right]/2\cdot\sigma^2}}{2\cdot\pi\cdot\sigma^2}$ has distribution of $r=(x^2+y^2)^{1/2}$, $f_r(r)=\frac{r}{\sigma^2}\cdot I_0\left(\frac{r\cdot\eta}{\sigma^2}\right)\cdot e^{-\left[r^2+\eta^2\right]/2\cdot\sigma^2}$, I_0 being the modified Bessel function, $r > 0$ [13] and $\bar{r}=\int_0^\infty r\cdot f_r(r)\,dr = 2\sqrt{2}e^{-\eta'^2}\sigma\int_0^\infty e^{-r'^2}\left[r'^2\, I_0(2r'\eta')\right]dr'$, where $r'=(r/\sqrt{2}\cdot\sigma)$ and $\eta'=(\eta/\sqrt{2}\cdot\sigma)$, e.g., evaluated by Hermite integration [14] (the mean of a non-central root χ^2 distribution approximated as ([14], pp. 943) $\{[2(\sigma+\eta)^2-(\sigma+2\eta)]/(\sigma+\eta)\}^{1/2}$ + $\mathrm{O}([\sigma+\eta]^{-3/2})$. The bias in the ratio of H_d's instantaneous and average envelope estimates (in A), to be subtracted from Figure 4's amplitude distortion correction array, depends on SNR, i.e., the H_d signal variance divided by the sum of R and noise (these two assumed having white spectra and Gaussian pdfs, e.g., for R by recourse to the central limit theorem) variances.

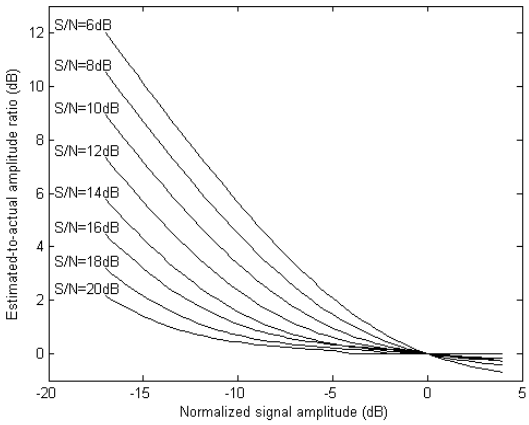

Figure 6. Bias in normalized H_d estimate (in A)

Finally, to minimize noise effects on the final map, the AM-normgain and AM-PM arrays are forced to least probability weighted[7] squares polynomial (e.g., for the nonlinear satellite channel, parabolic fits[8], $y=1-az^2$, $0<a<a_{max}$ and $\phi=bz^2$, $0<b<b_{max}$) of normalized envelopes.

[7] e.g., for unshaped 16-QAM, where $I=3$,

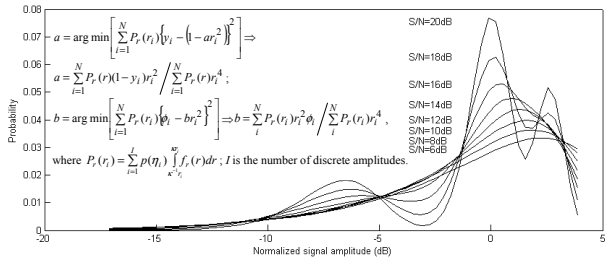

[8] Assuming parabolas accurately describe both amplitude and phase distortion, required IBO, so that inter-modulation products' spectral density (η in Figure 1) is below the noise floor, may approximately be obtained. Consider the noise-free distorted received signal $G_N(r)e^{j\phi(r)}\cdot[H(t)+\sum_{i=1}^{J}R_i(t)]\approx G_N(r)\cdot[1+j\phi(r)]\cdot[H(t)+\sum_{i=1}^{J}R_i(t)]$ ($\phi(r)<<1$). For $G_N(r)=1+ar^2$ and $\phi(r)=br^2$, $r^2=|H+S|^2=|H|^2+|S|^2+2\mathrm{Re}\{H^*S\}$, this is $G_N(r)e^{j\phi(r)}\cdot(H+\sum_{i=1}^{J}R_i)\approx[1+a|H|^2+a|S|^2+2a\,\mathrm{Re}(H^*S)]\cdot[1+jb|H|^2+jb|S|^2+2jb\,\mathrm{Re}(H^*S)]\cdot[H+S]$ When $|H|^2>>|S|^2$ is constant envelope, i.e., $|H|^2=C$, and all ab terms neglected, the echo-cancelled signal is $S+Ke^{j\Psi}\cdot\{2\mathrm{Re}(H^*S)\cdot(H+S)+CS\}$. The matched filtered output from the echo cancelled signal with the reference signal, $P(t)$, over the R_ith carrier's symbol duration, T_{Ri}, is:

$$\int_0^{T_{R_i}}\{R_i(t)P(t)\cdot\{1+KCe^{j\Psi}\}+2Ke^{j\Psi}S(t)P(t)\,\mathrm{Re}[H^*(t)S(t)]+2Ke^{j\Psi}\,\mathrm{Re}[H^*(t)S(t)]H(t)P(t)\}\cdot dt$$

Let $H(t)$ have carrier (w.r.t. $R_i(t)$) phase θ (a frequency offset between $H(t)$ and $R_i(t)$ causing a slow time varying θ); $H^I(t)=\sqrt{C}\cos(\theta+\theta_k)$, $H^I(t)=\sqrt{C}\sin(\theta+\theta_k)$, $k=n\pi/M_H$ for $n=0,1\ldots M_H-1$, i.e., M_H-ary PSK and for OFDM $\int_0^{T_{R_i}}R_m(t)P(t)\cdot dt=0$, $m\neq i$, to simplify, with $H_{C/N}=L\gamma R_{C/N}$, to:

$$\int_0^{T_{R_i}}\{R_i(t)P(t)\cdot\{1+2KCe^{j\Psi}\}+2Ke^{j\Psi}S(t)P(t)\,\mathrm{Re}[H^*(t)S(t)]\}+KCe^{j(\Psi+\theta)}\sum_{k=1}^{L\gamma}e^{j2\theta_k}\int_0^{T_{R_i}}S^*(t)P(t)\cdot dt$$

The inter-modulation term has variance $2K^2J^2C\sigma_{R_i}^2E_{b_{Ri}}$, which when divided by BW_{Ri} yields η, desired to be below N_0, i.e., $2K^2J^2C\sigma_{R_i}^2|R_i|^2/BW_{R_i}<N_0$; $N_0=\dfrac{\sigma_N^2}{BW_{R_i}}$ and $\left(\dfrac{\sigma_{R_i}^2}{\sigma_N^2}\right)=\dfrac{E_{b_{Ri}}\cdot BR_{R_i}}{N_o\cdot BW_{R_i}}$ (where BR_{Ri} is R_i's bit rate) makes the inequality $K^2<L\gamma\Gamma\left[2J^2C^2\log_2 M_R\cdot\left(E_{b_{Ri}}/N_0\right)_R\right]^{-1}$. When $L=32$, $\Gamma=1$, (with BR_{Ri}=64kbps and BR_H=2Mbps), γ =-3.3dB (i.e., $\left(\dfrac{E_b}{N_0}\right)_H$ =3.5dB for 2/3-coded 8-PSK and $\left(\dfrac{E_b}{N_0}\right)_R$ =5dB for ¾-coded M=16-QAM), $J=22$, leads to $K^2(C)<1.63\times10^{-3}C^{-2}$ and $\eta=\dfrac{2C^2K^2J^2R_i'}{L\gamma\Gamma}$ (where R_i' is R_i's power spectral density). For Figure 4's typical TWTA, the minimum IBO satisfying the inequality is 8dB, a practical back-off being 10-11dB.

3. FRACTIONAL SAMPLE ADAPTATION

Fractional sample time delay (of H') inclusion in adaptive filters is briefly discussed [15], the integer sample delay being initially obtained by an initial time delay estimation (e.g., by the FFT-based ambiguity function/ cross-correlation computation described in [6]) and subsequently tracking the integer sample closest to the adaptive filter's weight vector's centroid. Suppose that $H'_k\in Z^L$ is stationary zero-mean vector random process with autocorrelation matrix $\boldsymbol{\Omega}=E[H'_kH'_k{}^T]\ \forall k$, the reference signal, $A_k\in Z$, being a stationary zero-mean scalar random process and $w_k\in R^L$ is the weight vector at the kth time step. For this adaptive filter, the error is $\varepsilon_k=A_k-\Sigma w_k\cdot H'_k$, $w_k\in R^L$. Assume that H'_k and A_k are stationary with cross-correlation vector $\boldsymbol{p}=E[A_k\cdot H'_k]\ \forall k$. Using a MSE cost function $\xi=E|\varepsilon_k|^2=E|A_k|^2-2\boldsymbol{p}^T\boldsymbol{w}+\boldsymbol{w}^T\boldsymbol{\Omega}\boldsymbol{w}$, it is easily shown that for full rank $\boldsymbol{\Omega}$, the weight vector that minimizes ξ is $\boldsymbol{w}^{\mathrm{opt}}=\boldsymbol{\Omega}^{-1}\boldsymbol{p}$. The MSE when using $\boldsymbol{w}^{\mathrm{opt}}$ is denoted as ξ^{opt}. The Widrow-Hopf LMS algorithm [16] (Figure 7) estimates $\boldsymbol{w}^{\mathrm{opt}}$ when $\boldsymbol{\Omega}$ and $\boldsymbol{p}$ are unknown using an instantaneous error $|\varepsilon_k|^2$ via $w_{k+1}=w_k+2\mu\mathrm{Re}\{\varepsilon_kH'_k{}^*\}$, * connoting complex conjugate.

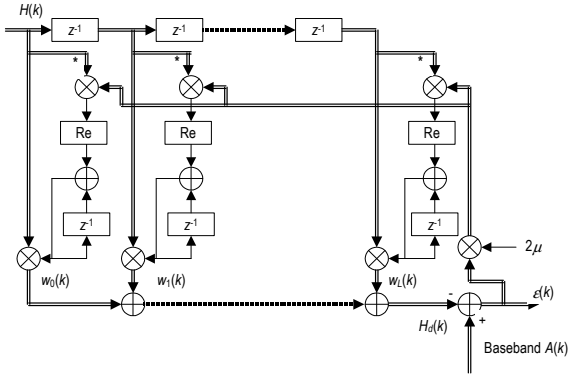

Figure 7. LMS fractional sample estimator

It has been shown [17] that, for large enough k, i.e., in steady state, for an arbitrary initial w_0, $E[w_k]=\boldsymbol{w}^{\mathrm{opt}}$ when $0<\mu\leq[3\mathrm{Tr}(\boldsymbol{\Omega})]^{-1}$, with w_k exhibiting Brownian motion around $\boldsymbol{w}^{\mathrm{opt}}$, the excess MSE (from [18]) being approximated by

$\xi_{excess}=\mu\xi^{opt}\mathrm{Tr}(\boldsymbol{\Omega})$. In [19] it is shown that it is preferable to separate the attenuation factor, α, of H_d in A (by multiplying A by $\sigma_H/(2\sigma_A)<\alpha^{-1}<\sigma_H/\sigma_A$) from the time delay adaptation.

The matrix $\boldsymbol{\Omega}$ of H'_k (for the outbound communication signal) is tri-diagonal when the signal is over-sampled by a factor less than 2. All principal diagonal terms being positive and greater than off-diagonal terms ensure $\boldsymbol{\Omega}$'s full rank, and thus, with $\mu\leq[3L\sigma_{H'}{}^2]^{-1}$, $\xi_{excess}=\mu\xi^{opt}L\sigma_{H'}{}^2$.

4. EXCESS ERROR WITH AND WITHOUT DISTORTION COMPENSATION

For uncompensated AM-Normgain distortion, $G_N(r)$, and phase distortion, $\phi(r)$, the error signal at amplitude, r, is $r\cdot[G_{LMS}\cdot e^{j\phi_{LMS}}-G_N(r)\cdot e^{j\phi(r)}]$; the overall reference normalized MSE is $\rho=\frac{\int_{r_{\min}}^{r_{\max}} f_r(r)\cdot r^2|G_{LMS}\cdot e^{j\phi_{LMS}}-G_N(r)e^{j\phi(r)}|^2dr}{\int_{r_{\min}}^{r_{\max}} f_r(r)\cdot r^2dr}$, where $f_r(r)$ is the pdf of r and G_{LMS} and ϕ_{LMS} are, respectively, the LMS gain (H in A is attenuated due to distortion) and constant phase shift minimizing MSE. First and second order Taylor series approximations of $e^{j[\phi(r)-\phi_{LMS}]}$, for small $|\phi(r)-\phi_{LMS}|$, are $1+j[\phi(r)-\phi_{LMS}]$ and $1-0.5[\phi(r)-\phi_{LMS}]^2+j[\phi(r)-\phi_{LMS}]$; the minimum normalized MSE in the two cases may be approximated by $\frac{\int_{r_{\min}}^{r_{\max}} f_r(r)\cdot r^2\{[G_{LMS}-G_N(r)]^2+G_N^2(r)\cdot[\phi(r)-\phi_{LMS}]^2\}dr}{\int_{r_{\min}}^{r_{\max}} f_r(r)\cdot r^2dr}$ and

$$\rho=\frac{\int_{r_{\min}}^{r_{\max}} f_r(r)\cdot r^2\cdot\left[(G_{bias}-G_N(r))^2+0.25\cdot(G_N(r)\cdot[\phi(r)-\phi_{bias}]^2)^2+[(\phi(r)-\phi_{bias})\cdot G_N(r)]^2+(G_{bias}-G_N(r))\cdot(G_N(r)\cdot[\phi(r)-\phi_{bias}]^2)\right]dr}{\int_{r_{\min}}^{r_{\max}} f_r(r)\cdot r^2\,dr}$$

which are evaluated in Appendices I, II and III.

The excess MSE without distortion compensation is approximately $\mu L\sigma_H^2\left(\alpha^2\rho G_{LMS}^2\sigma_H^2+\xi^{opt}\right)+\alpha^2\rho G_{LMS}^2\sigma_H^2$, while the excess error variance with distortion compensation is $\mu\cdot\xi^{opt}\cdot L\cdot\sigma_{H'}^2$. The excess error performance improvement with distortion compensation is approximately $\left(1+\frac{\alpha^2\rho\cdot G_{LMS}^2\cdot\sigma_H^2}{\xi^{opt}}+\frac{\alpha^2\rho\cdot G_{LMS}^2}{\mu\cdot\xi^{opt}\cdot L}\right)\sigma_H^2\Big/\sigma_{H'}^2$.

5. RESULTS

Figure 8 shows convergence and steady-state behaviors of the LMS fractional (in this case ½) sample estimator without (i), ideal (ii), best parabolic amplitude and phase distortion fits (iii) and adaptive (iv), distortion compensation. The signal component of H_d in A is attenuated by -20dB, while the residual signal, ξ^{opt}, is a further 20dB lower. Without distortion compensation, echo return loss enhancement (ERLE) is -29dB, while in case (iii) the ERLE is –32.5dB. For this example, distortion compensation also reduces excess noise by 5.1dB.

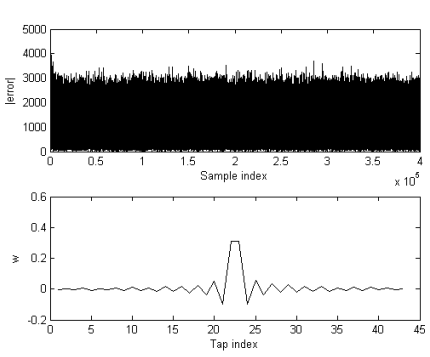

(i) σ_R=1387, ERLE=-29dB

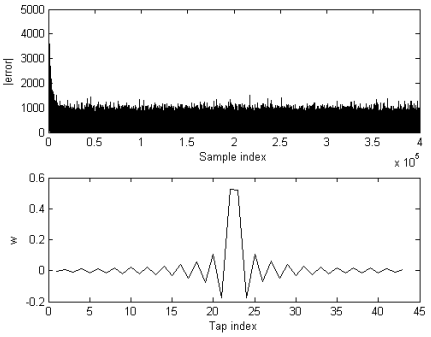

(ii) σ_R=312, ERLE=-39dB

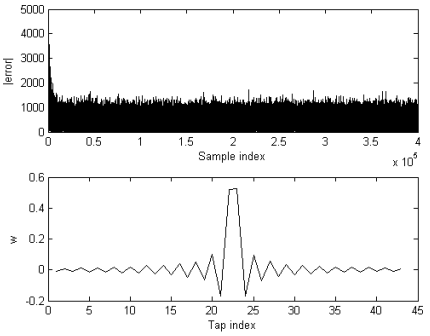

(iii) σ_R=394, ERLE=-35dB; with coefficients, a=-0.184 and b=0.297

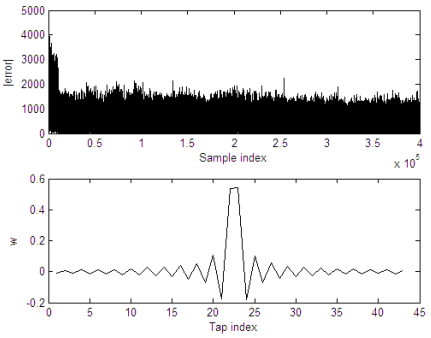

(iv) σ_R=427, ERLE varies between -28 to -37dB

Figure 8. μ=0.01/($L\sigma_{H'}{}^2$) fractional sample estimator convergence without (i), with ideal (ii), with parabolic fits (iii) and with adaptive (iv) distortion compensation (16-QAM -7dB IBO, normalized bandwidth=0.71).

6. CONCLUSION

An LMS echo canceller with distortion compensation has been described wherein:

- Amplitude and phase distortion characteristics are automatically acquired and tracked from the received signal (when echo dominates the received signal)
- Expressions for excess error with and without distortion compensation are obtained
- Distortion compensation is enabled when H/R exceeds a threshold

REFERENCES

[1] *ITU-T Recommendation G.165, Echo Cancellers*, ITU, Geneva, 1993.

[2] *ITU-T Recommendation G.167, Acoustic Echo Cancellers*, ITU, Geneva, 1993.

[3] A. Stenger, W. Kellerman and R. Rabenstein, "Adaptation of acoustic echo cancellers incorporating a memory-less non-linearity," *IEEE workshop on Acoustic Echo and Noise control*, Pocono Manor, PA, 1999.

[4] G.L. Sicuranza, "Quadratic Filters for Signal Processing," *Proc. IEEE*, vol. 80, pp. 1263-1285, 1992.

[5] P. Bondon and M. Krob, "Blind Identifiability of a Quadratic Stochastic System," *IEEE Trans. Inform. Theory*, vol. 41, No. 1, pp. 245-254, Jan. 1995.

[6] G.D. Collins, D.L. Anair and M.J. Ready, "Adaptive Canceller for Frequency Reuse Systems," US Patent 6,859,641 B2, February 22, 2005.

[7] R. De Gaudenzi and M. Luise, "Analysis and design of all-digital demodulator for trellis-coded 16-QAM transmission over a nonlinear satellite channel," *IEEE Trans. Commun.*, vol. COM-43, pp. 659-667, Feb.-Apr., 1995.

[8] S. Jayasimha and P. Jyothendar, "Kurtosis DPLL and PTCM decoder for non-linearly amplified 16-QAM," *Proc. of IEEE MILCOM-2005*, ISBN 0-7803-9394-5, *IEEE* catalog no. 05CH37719C.

[9] A. A. M. Saleh, "Frequency-independent and frequency-dependent nonlinear models of TWT amplifiers," *IEEE Trans. Commun.*, vol. COM-29, pp. 1715-1720, November, 1981.

[10] A. Ghorbani and M. Sheikhan, "The effect of Solid State Power Amplifiers (SSPAs) Nonlinearities on MPSK and M-QAM Signal Transmission", *Sixth Int'l Conference on Digital Processing of Signals in Comm*., 1991, pp. 193-197.

[11] R. Nee and R. Prasad, *OFDM for wireless multimedia communications*, Artech House Publishers, 2000.

[12] W.L. Pritchard *et. al.*, *Satellite Communication Systems Engineering*, Prentice Hall, NJ, 1993, pp. 413-418.

[13] A. Papoulis, *Probability, Random Variables and Stochastic Processes*, 3rd edition, McGraw Hill Inc. 1991, pp. 140.

[14] M. Abramowitz and I.A. Stegun, *Handbook of Mathematical Functions*, National Bureau of Standards, 1972, pp. 924 and pp. 943.

[15] T.I. Laakso, V. Valimaki, M. Karjalainen and U.K. Laine, "Splitting the Unit delay", *IEEE Sig. Proc. Magazine*, Jan. 1996.

[16] B. Widrow and M.E. Hopf, "Adaptive Switching Circuits," *IRE WESCON Conv. Rec.*, 1960, vol.4, pp. 96-104.

[17] A. Feuer and E. Weinstein, "Convergence analysis of LMS filters with uncorrelated Gaussian data," *IEEE Trans. ASSP*., vol. ASSP-33, no. 1, pp. 222-229, Feb. 1985.

[18] B.Widrow and S.D.Stearns, *Adaptive Signal Processing*, Prentice Hall, Upper Saddle River, NJ, 1985.

[19] X. Kong and V. Solo, "Effects of attenuation factor on adaptive time delay estimation," *ICASSP*-91, vol. 3, pp. 2121-2124, April 1991.

APPENDIX I

Setting $e^{j[\phi(r)-\phi_{LMS}]} \approx 1+j[\phi(r)-\phi_{LMS}]$, the overall MSE is the sum of the minimum (w.r.t. G_{LMS}) normalized MSE, $\rho_1 = \int_{r_{\min}}^{r_{\max}} f_r(r)\, r^2 [G_{LMS} - G_N(r)]^2 dr \Big/ \int_{r_{\min}}^{r_{\max}} f_r(r)\, r^2 dr$, were only amplitude distortion present, and the minimum (w.r.t. ϕ_{LMS}) normalized MSE term, $\rho_2 = \int_{r_{\min}}^{r_{\max}} f_r(r)\, r^2 G_N^2(r) [\phi(r) - \phi_{LMS}]^2 dr \Big/ \int_{r_{\min}}^{r_{\max}} f_r(r)\, r^2 dr$, the integral over r of weighted squares of amplitude-phase product,s where $G_{LMS} = \int_{r_{\min}}^{r_{\max}} f_r(r)\, r^2 G_N(r) dr \Big/ \int_{r_{\min}}^{r_{\max}} f_r(r)\, r^2 dr$, and $\phi_{LMS} = \int_{r_{\min}}^{r_{\max}} f_r(r)\, r^2 G_N^2(r) \phi(r) dr \Big/ \int_{r_{\min}}^{r_{\max}} f_r(r)\, r^2 G_N^2(r) dr$.

APPENDIX II

MSE with $e^{j[\phi(r)-\phi_{LMS}]} \approx 1\text{-}0.5[\phi(r)-\phi_{LMS}]^2 + j[\phi(r)-\phi_{LMS}]$ is:

$$\rho = \frac{\int_{r_{\min}}^{r_{\max}} f_r(r)\cdot r^2 \cdot \left[\left(G_{lms} - G_N(r)\right)^2 + 0.25\cdot \left(G_N(r)\cdot [\phi(r)-\phi_{lms}]^2\right)^2 + [(\phi(r)-\phi_{lms})\cdot G_N(r)]^2 + \left(G_{lms} - G_N(r)\right)\cdot \left(G_N(r)\cdot [\phi(r)-\phi_{lms}]^2\right)\right] dr}{\int_{r_{\min}}^{r_{\max}} f_r(r)\cdot r^2\, dr} \qquad \text{(AII-1)}$$

Minimizing MSE w.r.t. G_{LMS} and ϕ_{LMS} yields:

$A_1 G_{\mathrm{lms}} + B_2 \phi^2_{\mathrm{lms}} + B_1 \phi_{\mathrm{lms}} = K_1$ (AII-2)

$A_2 G_{\mathrm{lms}} + C_3 \phi^3_{\mathrm{lms}} + C_2 \phi^2_{\mathrm{lms}} + C_1 \phi_{\mathrm{lms}} + D G_{\mathrm{lms}} \cdot \phi_{\mathrm{lms}} = K_2$ (AII-3)

where

$$A_1 = 2\int_{r_{\min}}^{r_{\max}} f_r(r) r^2\, dr\,,\ B_2 = \int_{r_{\min}}^{r_{\max}} f_r(r) r^2 G_N(r) dr\,,\ C_3 = \int_{r_{\min}}^{r_{\max}} f_r(r) r^2 G_N^2(r) dr\,,$$

$$B_1 = -2\int_{r_{\min}}^{r_{\max}} f_r(r) r^2 G_N(r) \phi(r) dr\,,\ K_2 = \int_{r_{\min}}^{r_{\max}} f_r(r) r^2 G_N^2(r) \phi^3(r) dr$$

$$K_1 = 2\int_{r_{\min}}^{r_{\max}} f_r(r) r^2 G_N(r) dr - \int_{r_{\min}}^{r_{\max}} f_r(r) r^2 G_N(r) \phi(r)^2 dr \quad A_2 = -2\int_{r_{\min}}^{r_{\max}} f_r(r) r^2 G_N(r) \phi(r) dr\,,$$

$$C_2 = -3\int_{r_{\min}}^{r_{\max}} f_r(r) r^2 G_N^2(r) \phi(r) dr\,, \qquad C_1 = 3\int_{r_{\min}}^{r_{\max}} f_r(r) r^2 G_N^2(r) \phi^2(r) dr\,,$$

$D = 2\int_{r_{\min}}^{r_{\max}} f_r(r) r^2 G_N(r) dr$. Substitute (AII-2) in (AII-3) to obtain ϕ_{LMS} as a real root of the cubic equation $\phi^3_{\mathrm{lms}} + a_2 \phi^2_{\mathrm{lms}} + a_1 \phi_{\mathrm{lms}} + a_0 = 0$, where $a_2 = \frac{(C_2 A_1 - A_2 B_2 - D B_1)}{(C_3 A_1 - D B_2)}$, $a_1 = \frac{(C_1 A_1 - A_2 B_1 + D K_1)}{(C_3 A_1 - D B_2)}$ and $a_0 = \frac{(A_2 K_1 - K_2 A_1)}{(C_3 A_1 - D B_2)}$. Substitute ϕ_{LMS} in (AII-2) to obtain G_{LMS}, and then use (AII-1) to compute MSE.

APPENDIX III

The residual error estimate for noise-free unshaped 16-QAM (at -7dB IBO as in Figure 4) is ρ=0.016 for the first order Taylor series case (G_{LMS} =-2.93dB, ϕ_{LMS} =0.441rads, ρ_1=0.0063 and ρ_2=0.0097), while ρ=0.012 for the second order case (G_{LMS}=-2.98dB, ϕ_{LMS} =0.452rads).